

cAMP-specific phosphodiesterase HSPDE4D3 mutants which mimic activation and changes in rolipram inhibition triggered by protein kinase A phosphorylation of Ser-54: generation of a molecular model

Ralf HOFFMANN^{*1}, Ian R. WILKINSON^{*2,3}, J. Fraser McCALLUM^{*3}, Peter ENGELS^{†1} and Miles D. HOUSLAY^{*4}

^{*}Molecular Pharmacology Group, Division of Biochemistry and Molecular Biology, Davidson and Wolfson Buildings, IBLS, University of Glasgow, Glasgow G12 8QQ, Scotland, U.K., and [†]Novartis Pharma, Preclinical Research, 4002 Basel, Switzerland

Ser-13 and Ser-54 were shown to provide the sole sites for the protein kinase A (PKA)-mediated phosphorylation of the human cAMP-specific phosphodiesterase isoform HSPDE4D3. The ability of PKA to phosphorylate and activate HSPDE4D3 was mimicked by replacing Ser-54 with either of the negatively charged amino acids, aspartate or glutamate, within the consensus motif of RRES⁵⁴. The PDE4 selective inhibitor rolipram {4-[3-(cyclopentoxyl)-4-methoxyphenyl]-2-pyrrolidone} inhibited both PKA-phosphorylated HSPDE4D3 and the Ser-54 → Asp mutant, with an IC₅₀ value that was ~8-fold lower than that seen for the non-PKA-phosphorylated enzyme. Lower IC₅₀ values for inhibition by rolipram were seen for a wide range of non-activated residue 54 mutants, except for those which had side-chains able to serve as hydrogen-bond donors, namely the Ser-54 → Thr, Ser-54 → Tyr and Ser-54 → Cys mutants. The Glu-53 → Ala mutant exhibited an activity comparable with that of the PKA phosphorylated native enzyme and the Ser-54 → Asp mutant but, in contrast to the native enzyme, was insensitive to activation by PKA, despite being more rapidly phosphorylated

by this protein kinase. The activated Glu-53 → Ala mutant exhibited a sensitivity to inhibition by rolipram which was unchanged from that of the native enzyme. The double mutant, Arg-51 → Ala/Arg-52 → Ala, showed no change in either enzyme activity or rolipram inhibition from the native enzyme and was incapable of providing a substrate for PKA phosphorylation at Ser-54. No difference in inhibition by dipyrindamole was seen for the native enzyme and the Ser-54 → Asp and Ser-54 → Ala mutants. A model is proposed which envisages that phosphorylation by PKA triggers at least two distinct conformational changes in HSPDE4D3; one of these gives rise to enzyme activation and another enhances sensitivity to inhibition by rolipram. Activation of HSPDE4D3 by PKA-mediated phosphorylation is suggested to involve disruption of an ion-pair interaction involving the negatively charged Glu-53. The increase in susceptibility to inhibition by rolipram upon PKA-mediated phosphorylation is suggested to involve the disruption of a hydrogen-bond involving the side-chain hydroxy group of Ser-54.

INTRODUCTION

Cells balance the hormone-driven synthesis of the second messenger cAMP by adenylate cyclase with the degrading activity of the cyclic nucleotide phosphodiesterases [1]. These cyclic nucleotide phosphodiesterases have, to date, been classified into seven families according to their substrate specificity, sequence similarities and regulatory sites [1–9].

Members of the PDE4 (type IV) phosphodiesterase family exclusively hydrolyse cAMP and are selectively inhibited by the anti-depressant, rolipram {4-[3-(cyclopentoxyl)-4-methoxyphenyl]-2-pyrrolidone} [3,4,6,9–11]. Four genes (A, B, C, D) encode different PDE4 isoenzymes, with the complexity of the protein products being increased by alternate splicing [10]. This yields multiple splice variants produced by every gene. Such findings imply a role for distinct PDE4 isoforms in determining a number of specific, tightly controlled functions involved in the regulation of cellular cAMP levels. There is considerable interest

in developing therapeutics to inhibit selectively specific PDE classes. Indeed, selective inhibitors of PDE4 enzymes can serve as anti-inflammatory agents and have potential as therapeutic agents in a wide range of disease states, including asthma [6,9,10,12,13]. However, the breadth of PDE4 isoforms found in cells makes it imperative to appreciate the role of specific forms, their regulation and the molecular basis of altered susceptibility [6,12] of certain isoforms to inhibition by the PDE4 selective inhibitor, rolipram.

The central coding regions of the various PDE4 genes show high sequence similarity to each other and are believed to encode the catalytic domain [3,4,10]. At the N-terminal side of this region are two further regions of similarity which serve as unique signatures of the PDE4 enzyme families. These are known as the upstream conserved regions, UCR1 and UCR2, which are separated from each other and the catalytic unit by the linker regions, LR1 and LR2 [10]. In contrast, the alternatively spliced N-terminal regions show little similarity and have been suggested

Abbreviations used: DMEM, Dulbecco's modified Eagle's medium; FCS, fetal calf serum; PDE, cyclic nucleotide phosphodiesterase (EC 3.1.4.17); PDE4, rolipram-inhibited cAMP-specific PDE family; HSPDE4D, human PDE4 sub-family D with isoforms characterized by numerals; HSPDE4D3, human PDE4D isoform (GenBank deposition number L20970); rolipram, 4-[3-(cyclopentoxyl)-4-methoxyphenyl]-2-pyrrolidone; UCR, upstream conserved region; PKA, cAMP-dependent protein kinase (protein kinase A); mAb, monoclonal antibody; VSV, vesicular stomatal virus.

¹ Present address: BioFrontiera Pharmaceuticals GmbH, GIZ Hemmelratherweg 201 51377, Leverkusen, Germany.

² Present address: Department of Biochemistry, University of Sheffield, Sheffield, U.K.

³ These two authors contributed equally to this work.

⁴ To whom correspondence should be addressed (e-mail M.Houslay@bio.gla.ac.uk).

to contribute to the distinct pattern of intracellular targeting seen for certain isoforms, as well as conferring specific regulatory functions on particular isoforms [1,3,4,10,14,15]. The two major splice junctions which characterize the PDE4 gene families lead to the production of two classes of splice variants, the so-called 'long' forms which have both UCR1 and UCR2 and the 'short' forms which have only UCR2 [3,4,10].

Five distinct splice variants produced from the PDE4D gene have been shown to exist in man and rat at the level of both DNA transcription and protein expression [4,16–21]. Two short (PDE4D1, 2) and three long (PDE4D3, 4, 5) forms of PDE4D have been described which are characterized by N-terminal variation [18,20,22]. The rat PDE4D3 isoform is a long PDE4D product which has been shown to become activated in intact cells as a consequence of a hormone-stimulated increase of intracellular cAMP [3,20,21,23]. *In vitro* modification studies, done in cell lysates treated with protein kinase A (PKA), have demonstrated the activation and phosphorylation of both the rat and human forms of PDE4D3 [3,20,21,23]. Such activation was apparent at saturating substrate concentrations, implying a change in V_{max} with no effect on the K_m for cAMP. There are two potential PKA phosphorylation sites in PDE4D3, namely Ser-13 and Ser-54, and selective mutation of these residues to alanine in rat PDE4D3 has demonstrated that PKA can phosphorylate PDE4D3 at both of these sites [23]. Nevertheless, only the Ala-54 mutant failed to become activated as a consequence of PKA action, implying that modification at this site led to increased catalytic activity. However, it was unclear from such studies [23,24] whether PKA was able only to activate a sub-population of PDE4D3 which had heightened sensitivity to inhibition by rolipram, or whether PKA-mediated phosphorylation itself elicited an increase in sensitivity to inhibition rolipram. We address this outstanding question here using a variety of mutant forms of human PDE4D3 which have allowed us to dissociate the conformational change which causes enzyme activation by PKA from that which confers an increased susceptibility to inhibition by rolipram.

MATERIALS AND METHODS

Protein concentration was determined according to the method of Bradford using BSA as the standard [25]. Sequencing was done on an automated sequencing machine (ABI model 373 or 377; Perkin-Elmer) with assays containing 1.5 μ g of plasmid DNA and 15 pmol of appropriate sequencing oligonucleotide (DNA sequencing kit, Dye Terminator Cycle Sequencing Ready Reaction; Perkin-Elmer). All PCRs were done in a volume of 25–50 μ l. Standard PCR reaction mixtures contained 200 μ M dNTP, 20 pmol of each oligonucleotide, 50–100 ng of DNA template and 0.2–1 unit of Taq DNA polymerase. SDS/PAGE was performed according to the method of Laemmli [26].

DNA constructs

A cDNA encoding the human phosphodiesterase type 4D3 (HSPDE4D3) was isolated by reverse transcriptase PCR from neuroblastoma cells as described previously [27] and cloned into the *EcoRV* cloning site of pBluescript. Subcloning into the expression vector pCIneo (Promega) was performed by PCR with KlenTaq-polymerase (Clontech) using the following oligonucleotides: 5'-end: 5'-CGGAATTCCGATGATGCACGTG-AATAAT-3', 3'-end: 5'-GCTCTAGAAAACCGGTGTCAGG-AGAACGATCATC-3'. These include overhanging restriction sites for *EcoRI*, *XbaI* and *AgeI*. The PCR product was purified, digested with *EcoRI* and *XbaI* and subcloned into the cor-

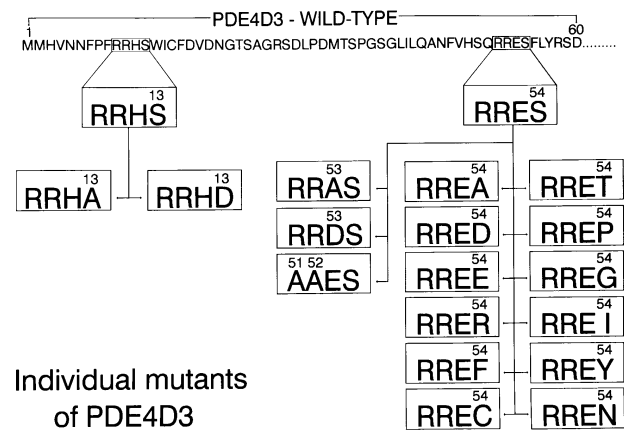


Figure 1 Schematic diagram of the various mutant forms of HSPDE4D3

The generation of these mutants is detailed in the Materials and methods section.

responding restriction sites of pCIneo, generating the plasmid pCI-HSPDE4D3. Two 5'-phosphorylated complementary oligonucleotides coding for the vesicular stomatal virus (VSV) epitope [28] followed by a translation stop signal were constructed for generating overhanging *AgeI* and *SalI* restriction sites after hybridization. The nucleotide sequence of this construct, which includes the *AgeI* site, *EcoRV* site and *SalI* sites is 5'-AAAA-CCGGTTACACCGATATCGAGATGAACAGGCTGGGA-AAGTGAGTCTGACTCG-3'. This creates a C-terminal VSV epitope [28] of amino acid sequence Tyr-Thr-Asp-Ile-Leu-Met-Asn-Arg-Leu-Gly-Lys-STOP. The small DNA fragment was subcloned, in frame, into *AgeI/SalI*-digested pCI-HSPDE4D3, giving the expression plasmid pCI-HSPDE4D3-VSV. Correct cDNA amplification via PCR was analysed by sequencing.

Site-directed mutagenesis of HSPDE4D3

The various mutants at and around positions 13 and 54 in HSPDE4D3 are shown schematically in Figure 1. Replacement of the amino acid serine at position 13 in HSPDE4D3 by either an alanine or an aspartate residue was performed by a PCR procedure using the oligonucleotides 5'-CGGAATTCCGATG-ATGCACGTGAATAATTTTCCCTTTAGAAGGCATGCC-TGG-3' to yield Ala-13, and 5'-CGGAATTCCGATGATGCA-CGTGAATAATTTTCCCTTTAGAAGGCATGACTGG-3' to yield Asp-13, where the changed nucleotide triplet is underlined.

The PCR reaction profile with KlenTaq polymerase (Clontech) was 95 °C for 3 min, 45 s at 95 °C, 45 s at 55 °C, 90 s at 72 °C for 35 cycles, followed by an extension for 90 s at 72 °C. A PDE4D3 internal primer provided the second oligonucleotide in the PCR reaction, namely 5'-CAAATCAGCCAGTAGATTCATGTG-3'. This allowed for the generation of corresponding PCR fragments of 1.4 kb. Such PCR products were digested with *EcoRI* and *BclI* and introduced into *EcoRI/BclI*-digested pCI-HSPDE4D3-VSV.

In order to change Ser-54 to Ala in HSPDE4D3, PCR extension with KlenTaq polymerase was used in the first PCR reaction together with the oligonucleotides: 5'-CGGAATTCC-GATGATGCACGTGAATAATTTTCCC-3' and 5'-ATACA-GGAAGGCCTCCCGTCGTTG-3'.

The profile employed 95 °C for 3 min, 45 s at 95 °C, 45 s at

55 °C, 30 s at 72 °C for 35 cycles, followed by an extension for 30 s at 72 °C. In the second PCR reaction the primers employed were: 5'-CAACGACGGGAGGCCTTCTGTAT-3' and 5'-CAAATCAGCCAGTAGATTCATGTG-3'.

The amplification protocol employed was 95 °C for 3 min, 45 s at 95 °C, 45 s at 55 °C, 60 s at 72 °C for 35 cycles, followed by an extension for 60 s at 72 °C. This was followed by a third amplification reaction with a 1:1 mixture of 5 µl of PCR reaction mixtures 1 and 2, each with the oligonucleotides: 5'-CGGAAT-TCCGATGATGCACGTGAATAATTTTCCC-3' and 5'-CAA-ATCAGCCAGTAGATTCATGTG-3'.

The amplification protocol employed was 95 °C for 3 min, 45 s at 95 °C, 45 s at 55 °C, 90 s at 72 °C for 35 cycles, followed by an extension for 90 s at 72 °C. The extended PCR fragment of 1.4 kb was digested with the enzymes *EcoRI* and *BclI*. A corresponding 1 kb fragment was purified and subsequently introduced into *EcoRI/BclI*-digested pCI-HSPDE4D3-VSV. The same procedure was performed to allow for the mutation of Ser-54 to Asp-54, but using in the first PCR reaction: 5'-CGGAATTCGATGATGCACGTGAATAATTTTCCC-3' and 5'-ATACAGGAAGTCTCCCGTCGTTG-3', and in the second PCR-reaction: 5'-CAACGACGGGAGGACTTCCTG-TAT-3' and 5'-CAAATCAGCCAGTAGATTCATGTG-3'. In the third PCR reaction a 1:1 mixture of 5 µl of each of these two PCR reactions was used together with the oligonucleotides 5'-CGGAATTCGATGATGCACGTGAATAATTTTCCC-3' and 5'-CAAATCAGCCAGTAGATTCATGTG-3'.

The extended PCR fragment of 1.4 kb was digested with *EcoRI* and *BclI* and the purified corresponding 1 kb fragment was introduced into *EcoRI/BclI*-digested pCI-HSPDE4D3-VSV.

The double mutants Ala-13/Ala-54 and Asp-13/Asp-54 were constructed by introducing either an alanine or an aspartate at amino acid position 13 into the existing mutants Ala-54 and Asp-54, as described above for wild-type HSPDE4D3.

The serial mutations of Ser-54 to the amino acids glutamate, arginine, phenylalanine, cysteine, threonine, proline, glycine, tyrosine and isoleucine of HSPDE4D3 was done using the 'QuikChange' Site-Directed Mutagenesis Kit from Stratagene Cloning Systems (La Jolla, CA, U.S.A.) according to the instructions of the manufacturer. The following oligonucleotides pairs (i, ii) for the individual mutants were used:

Glu-54: (i)

5'-GTCCACagccaaCGACGGGAGGAATTCCTGTATCGA-TCC-3'

(ii)

5-GGATCGATACAGGAATTCCTCCCGTCGttgctGTGG-AC-3'

Arg-54: (i)

5'-GTCCACagccaaCGACGGGAGCGCTTCCTGTATCGA-TCC-3'

(ii)

5'-GGATCGATACAGGAAGCGCTCCCGTCGttgctGTG-GAC-3'

Phe-54: (i)

5-GTCCACagccaaCGACGGGAGTTCCTTCCTGTATCGA-TCC-3'

(ii)

5'-GGATCGATACAGGAAGAACTCCCGTCGttgctGTG-GAC-3'

Cys-54: (i)

5'-GTCCACagccaaCGACGGGAGTGCCTTCCTGTATCGA-TCC-3'

(ii)

5'-GGATCGATACAGGAAGCACTCCCGTCGttgctGTG-GAC-3'

Thr-54: (i)

5'-GTCCACagccaaCGACGGGAGACCTTCCTGTATCGA-TCC-3'

(ii)

5'-GGATCGATACAGGAAGGTCTCCCGTCGttgctGTG-GAC-3'

Pro-54: (i)

5'-GTCCACagccaaCGACGGGAGCCCTTCCTGTATCGA-TCC-3'

(ii)

5'-GGATCGATACAGGAAGGGCTCCCGTCGttgctGTG-GAC-3'

Gly-54: (i)

5'-GTCCACagccaaCGACGGGAGGGCTTCCTGTATCGA-TCC-3'

(ii)

5'-GGATCGATACAGGAAGCCCTCCCGTCGttgctGTG-GAC-3'

Ile-54: (i)

5'-GTCCACagccaaCGACGGGAGATCTTCCTGTATCGA-TCC-3'

(ii)

5'-GGATCGATACAGGAAGATCTCCCGTCGttgctGTG-GAC-3'

Tyr-54: (i)

5'-GTCCACagccaaCGACGGGAGTACTTCCTGTATCGA-TCC-3'

(ii)

5'-GGATCGATACAGGAAGTACTCCCGTCGttgctGTG-GAC-3'

Changed nucleotide codons are underlined and the silent mutation for deletion of the restriction site for the endonuclease *HindII*, encoded by the wild-type PDE4D3 at nucleotide position -15 to -10 relative to the mutated triplet, is in lower case. Transformants were pre-screened for the deleted *HindII* restriction site by a PCR procedure. In this procedure, an aliquot from the transformed cells was directly introduced into 25 µl of standard PCR reaction mixture containing 0.2 units of Taq-polymerase (Pharmacia). The oligonucleotides used were: 5'-ATGATGCACGTGAATAATTTTCCCTTTAG-3' and 5'-AG-ACTGGACAACATCTGCAGCATG-3'. These resulted in a 1 kb PCR product being produced by the PCR reactions. Such species were directly digested by the addition of 5 units of the endonuclease *HindII* followed by an incubation for 2 h at 37 °C. Plasmid DNA was prepared from bacterial colonies which showed undigested PCR products on agarose gels, and was then sequenced in order to confirm the correct mutation.

Cell culture

The SV40-transformed monkey kidney cell line COS1 was cultured at 37 °C in an atmosphere of 5% CO₂/95% air in complete growth medium containing Dulbecco's modified Eagle's medium (DMEM) supplemented with 0.1% penicillin/streptomycin (10000 units/ml) and 10% (v/v) fetal calf serum (FCS). The day before transfection, cells were plated at a density of 5 × 10⁵ cells per 9-cm-diameter plate. For transfection, cells were overlaid with 5 ml of DMEM containing 10% (v/v) Nu-serum and 0.1 mM chloroquine. Plasmid DNA (20 µg) was diluted to 250 µl with TE-buffer [10 mM Tris/HCl (pH 8.0)/1 mM EDTA] mixed with 200 µl of DEAE-Dextran (10 mg/ml) and incubated for 15 min at room temperature. The DNA solution was dropped onto the cells and mixed with the medium by swirling. Cells were incubated for 4 h at 37 °C. The transfection medium was aspirated and the cells were shocked with 10%

DMSO in PBS for 2 min at room temperature. The monolayer was then washed twice with 5 ml of PBS and subsequently incubated in DMEM containing 10% (v/v) FCS. After 24 h at 37 °C in 5% CO₂/95% air, the cells were transferred to new plates and cultured for another 24 h at 37 °C in 5% CO₂/95% air.

Preparation of cell extracts

Forty-eight hours post-transfection, cell monolayers were washed once with PBS and scraped from the culture dish in 1 ml PBS per 9-cm plate, collected by centrifugation and resuspended in 200 µl of PDE extraction buffer [20 mM Tris/HCl (pH 7.5)/20% (v/v) glycerol/15 mM 2-mercaptoethanol/50 mM NaCl/5 mM EDTA/0.1% Triton X-100 supplemented with 1 mM dithiothreitol and a mixture of protease inhibitors at a final concentration of 40 µg/ml PMSF, 156 µg/ml benzamide and 1 µg/ml each of aprotinin, leupeptin, pepstatin A and antipain]. Cells were sonicated (Branson sonifier microtip) and then centrifuged for 5 min at 14000 *g*_{av}. The supernatant was then analysed for the presence of VSV-tagged protein by immunoblotting using a specific monoclonal antibody (mAb), as described by others in detail [28,29], and also for cAMP phosphodiesterase activity.

Western-blot analysis

Acrylamide gels (10%) were used and the samples boiled for 3 min after being resuspended in Laemmli [26] buffer. Gels were run at 8 mA/gel overnight or 50 mA/gel for 4–5 h with cooling. For detection of transfected PDE by Western blotting, ~20 µg of protein samples were separated by SDS/PAGE and then transferred to nitrocellulose. Membranes were blocked with 10% (w/v) low-fat milk powder in PBS overnight at 4 °C. They were then incubated in diluted anti-VSV monoclonal antibody (1:500 in PBS containing 0.5% milk powder) for 1–2 h at room temperature. Detection of bound antibody was carried out with anti-mouse-IgG peroxidase-conjugated secondary antibody (Sigma) using the enhanced chemiluminescence (ECL) detection system. After 1 min of incubation in ECL reagents at room temperature membranes were exposed to ECL hyperfilms.

Immunoprecipitation

Cell lysate from 5×10^5 transfected COS1-cells was incubated with 3–5 µl of monoclonal anti-VSV antibodies for 60 min on ice, followed by 30 min at room temperature. Antigen–antibody complexes were bound to 30 µl of protein G-coupled fast flow Sepharose for 60 min at room temperature. The immobilized material was collected by centrifugation, washed three times with 1 ml of PDE buffer (20 mM Tris/HCl, pH 7.7, 1 mM MgSO₄, 15 mM 2-mercaptoethanol) followed by three wash cycles with 1 ml of PDE buffer containing 0.5% Triton X-100 and 50 mM NaCl. A further wash cycle was performed with 1 ml of PDE buffer and the Sepharose gel pellet was finally resuspended in PDE buffer.

PKA assay

Assays for protein kinase activity were performed in a volume of 40 µl of a mixture containing 20 mM Tris/HCl (pH 7.5), 10% (v/v) glycerol, 15 mM 2-mercaptoethanol, 0.1 mM [γ -³²P]ATP (100 MBq/mmol), 5 mM MgCl₂ and 10 µM of the heptapeptide PKA substrate Kemptide. Samples were warmed to 30 °C and incubation was started by the introduction of the protein kinase. At different time points, 20 µl aliquots of the reaction mixture were spotted onto 2 × 2 cm squares drawn in a 'chessboard-like'

manner on Whatman P-81 phosphocellulose paper. After completion of a series of assays the paper sheet was washed by gentle shaking in 30% acetic acid for 5 min, followed by three washes in 15% acetic acid for 10 min each. Subsequently the paper was dried at 100 °C, the squares were then cut out and counted individually in a vial containing scintillation mixture.

PDE assays

PDE activity was determined by a modification of the two-step procedure of Thompson and Appleman [30] and Rutten et al. [31] as described previously by Marchmont and Houslay [32]. All assays were conducted at 30 °C and in all experiments a freshly prepared slurry of Dowex/H₂O/ethanol (1:1:1) was used for determination of activities. Initial rates were taken from linear time-courses of activity and activity was linear with added protein concentration over the ranges used. For the determination of kinetic parameters, the PDE assays were conducted using 10–15 different cAMP concentrations over a range from 0.1 µM to 100 µM. Dose-dependent inhibition by rolipram was determined in the presence of 1 µM cAMP and over a range (at least 16 different values; 0.1 nM–50 µM) of rolipram concentrations. IC₅₀ values were determined by a non-iterative curve-fitting procedure using the Kaleidagraph Package on an Apple Macintosh Computer as described previously [33]. The transfection procedure utilized in the present study led to high levels of novel PDE4 activity being produced, such that this comprised > 97% of the total COS cell PDE activity. Mock transfections, with vector only, as indicated in previous studies [34–37], did not alter the endogenous COS cell PDE activity. As a routine, however, we subtracted the residual endogenous COS-1 cell PDE activities done in parallel experiments from those activities found in the PDE4D-transfected cells. Representative studies were also performed on PDE4D species immunoprecipitated using the anti-VSV mAb, with identical results being obtained. Protein was routinely measured by the method of Bradford [25] using BSA as a standard.

In some instances PDE activity was assayed using scintillant cAMP-binding beads (PDE SPA kit; Amersham) at 22 °C following the manufacturer's protocol. Linearity of the reaction was checked by determining the PDE activity of each sample at several time points. In typical assays, 5–10 µl of a lysate from 5×10^5 transfected COS-1 cells were tested in a 50-fold dilution. The activity was normally in the range of 500–1000 pmol cAMP hydrolysed per min per mg of protein. cAMP PDE activity of untransfected COS-1 cells was about 50 to 100-fold lower under these conditions. Similar results were obtained using both procedures.

Relative specific PDE activity values for the various mutant forms were determined essentially as described previously [34,35,37]. First, the relative levels of expression of each of the particular PDE4D3 species in the various transfection experiments was determined immunologically. This was achieved by analysing increasing concentrations of protein (2–100 µg) from transfected COS-1 cells using either an ECL technique or by an ELISA technique as described in detail previously [34,35,37,38]. Scanning of signals on ECL hyperfilms was performed with a computing densitometer (Molecular Dynamics) with quantification done using ImageQuant software (Molecular Dynamics). Analyses were done over a range where the measured signal intensity was linear with respect to protein concentration [33,34,37]. In some instances an ELISA method [38] was used to quantify VSV immunoreactivity. Similar results were obtained using both procedures, which allowed plots of absorbance against micrograms of sample protein applied to be generated in order to

gauge the relative concentrations of particular PDE4D3 forms in different transfection experiments. Such data allowed us then to gauge the specific enzyme activities of the various mutant PDE4D3 forms relative to that of the wild-type enzyme.

Phosphorylation of PDE4D3

HSPDE4D3 from 5×10^5 transfected COS-1 cells was immunoprecipitated as described above using the anti-VSV mAb. The PDE complexed to the protein G-Sepharose was incubated for 30 min at room temperature with 1 vol. of PKA buffer (100 mM Tris/HCl (pH 7.5)/0.2 mM ATP/10 mM $MgCl_2$ /30 mM 2-mercaptoethanol/20% glycerol supplemented with the PKA inhibitor H89 at a concentration of 1 μ M]. This pre-incubation was done in order to militate against any ^{33}P -labelling of the PDE4D3 by any protein kinases which might potentially contaminate the preparation and thus cause ^{33}P -labelling independent of PKA action. Thus, by first pre-incubating the immunoprecipitates with unlabelled ATP in the presence of the potent PKA inhibitor H89, we aimed to allow any such phosphorylation to occur with unlabelled ATP, while preventing any modification of these enzymes by PKA. The immunoprecipitates were then washed three times with 1 ml of PDE buffer in order to remove the H89. The action of added PKA was then ascertained by resuspending the pelleted material in 1 vol. of PKA buffer containing 0.1 mM [γ - ^{33}P]ATP (100 MBq/mmol) and 10 μ M okadaic acid. The enzyme reaction was started by introduction of 1 μ -unit of catalytic subunit of PKA and allowed to continue for 30 min at room temperature, unless stated otherwise. The Sepharose was washed four times with 1 ml of PDE buffer and resuspended in PDE buffer for analysis.

Metabolic labelling of human PDE4D3 with [^{33}P]orthophosphate

Transfected COS1-cells (5×10^5) were subdivided after 24 h of cultivation into 6-well tissue-culture plates and incubated at 37 °C in 5% CO_2 /95% air for another day. The culture medium was aspirated, followed by a wash with phosphate-free DMEM medium and covering of the monolayer with 350 μ l/well of labelling medium containing phosphate-free DMEM, 2% (v/v) dialysed FCS, 20 mM Hepes, pH 7.4, the indicated enzyme inhibitors and 100 μ Ci of [^{33}P]orthophosphate. Cells were incubated overnight under standard conditions. The labelling medium was discarded, cells were washed twice with PBS and subsequently disrupted in a cell culture lysis buffer (Clontech) supplemented with 10 μ M okadaic acid. Radiolabelled PDE4D3 was immunoprecipitated as described above and then subjected to SDS/PAGE and autoradiography.

Time course phosphorylation PDE4D3 wild type and A53-mutant

COS-1 cells were transfected so as to express VSV epitope-tagged HSPDE4D3 as described above. Cell extracts were checked for the concentration of both the wild-type HSPDE4D3 and Ala-53 mutant by immunoblotting cell extracts with anti-VSV antibody. Equal amounts of immunoreactive material of both the wild-type HSPDE4D3 and Glu-53 \rightarrow Ala mutant were immunoprecipitated as described above. The protein G-Sepharose-adsorbed fractions for each of these enzyme preparations were split into six fractions which all contained the same amount of immunoreactive, gel-bound wild-type HSPDE4D3 and Glu-53 \rightarrow Ala mutant. Each of these fractions was incubated with PKA and [γ - ^{33}P]ATP, as described above, for the indicated times over a 45 min period. The phosphorylation reaction was stopped by washing the Sepharose with 1 ml of ice-cold PDE buffer, addition of SDS gel-loading buffer and boiling the sample for

5 min. Samples were run on an SDS gel and measured for phosphate incorporation using a PhosphorImager. Radioactivity was determined as counts per min (c.p.m.) at different time points.

RESULTS

Expression of VSV epitope-tagged HSPDE4D3 in COS1-cells

In these studies we wished to be able to analyse phosphorylated and mutant forms of PDE4D3 free of any possible contamination of endogenously expressed PDE4D species that might be found in COS-1 cells. This is of particular importance in phosphorylation studies where we wished to determine whether Ser-13 and Ser-54 were the only sites of PKA phosphorylation and thus such analyses would be prejudiced by the use of PDE4D antisera which would also immunoprecipitate any native PDE4D species. To obviate this we chose to use an epitope-tagged version of HSPDE4D3 which allowed us to immunoprecipitate the recombinant enzymes selectively for analyses. We chose to place a small epitope tag at the C-terminus of PDE4D3, as current evidence indicates that this would be unlikely to alter enzyme properties [10,39]. We thus employed in these studies both an unmodified recombinant human PDE4D3 enzyme [27] and one [18] with an epitope-tag coding for 11 C-terminal amino acids of VSV glycoprotein [28] targeted to the C-terminus of HSPDE4D3.

Produced in transfected COS-1 cells, VSV-tagged HSPDE4D3 migrated as a single immunoreactive species of apparent size 96 ± 3 kDa ($n = 3$; mean \pm S.D.) on SDS/PAGE (Figure 2). Such a VSV-tagged species has been shown [18] to migrate on SDS/PAGE similarly to that of its naturally occurring counterpart (95 ± 3 kDa; $n = 3$; mean \pm S.D.) when analysed under identical conditions. The detection of tagged HSPDE4D3 enzyme was achieved with mAbs that recognize the five C-terminal residues of VSV glycoprotein [28,29]. The Ser-54 \rightarrow Ala and Ser-54 \rightarrow Asp mutants of the epitope-tagged HSPDE4D3 also migrated similarly to the wild-type enzyme upon SDS/PAGE (Figure 2).

The PDE activity (assayed at 1 μ M cAMP) of cell cytosol extracts expressing recombinant VSV-tagged HSPDE4D3 was in the region of 800 ± 6 pmol/min per mg of protein ($n = 3$; mean \pm S.D.), compared with 'vector-only' transfected cells which exhibited a PDE activity of 20 ± 4 pmol/min per mg of protein ($n = 3$; mean \pm S.D.), indicating that $> 97\%$ of the activity was due to recombinant HSPDE4D3. Use of a polyclonal

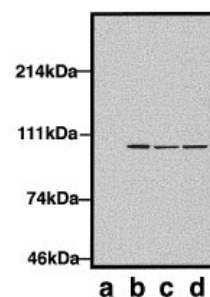


Figure 2 Immunodetection of epitope-tagged HSPDE4D3

Typical immunoblot of an SDS/PAGE gel analysing vector-only transfected COS1 cells (lane a) and COS cells transfected to express VSV epitope tagged forms of wild-type HSPDE4D3 (lane b) and its Ser-54 \rightarrow Asp (lane c) and Ser-54 \rightarrow Ala (lane d) mutants. Results are typical of experiments done three times.

Table 1 Relative activity and rolipram inhibition of HSPDE4D3 mutants

IC₅₀ values for inhibition by racemic rolipram were determined using 1 μM cAMP as substrate, as specified in the Materials and methods section. The K_m value for cAMP hydrolysis by the VSV-tagged native form of HSPDE4D3 was 1.1 ± 0.2 μM, which is very similar to that of the non-tagged recombinant enzyme expressed in COS1 cells (0.9 ± 0.3 μM) and the recombinant HSPDE4D3 [27] expressed in *Saccharomyces cerevisiae* (1.7 ± 0.3 μM). The various mutants examined here exhibited similar K_m values for cAMP hydrolysis, lying in the range 0.99–1.15 μM. Thus the changes in IC₅₀ values recorded here for certain of the mutant HSPDE4D3 forms reflect alterations in the binding of the inhibitor to the enzyme forms. PDE activity is expressed relative to that of the wild-type form of HSPDE4D3 (given a value of 1) using equal amounts of enzyme protein as detected immunologically. Results are shown for three distinct transfection studies with means ± S.D. given (*n* = 3). n.d., not determined. Data were analysed by Student's *t*-test with †not significant, ****P* < 0.001, ***P* < 0.01, **P* < 0.05 compared with the values for the wild-type enzyme. 'Status' indicates the grouping of the mutants with regard to PDE activity compared with the wild-type enzyme (activated, non-activated, inhibited) and rolipram inhibition (shifted to a lower IC₅₀ value or non-shifted).

Status	HSPDE4D3 species	Specific activity relative to wild-type enzyme	Rolipram IC ₅₀ value (μM)
Standard	Wild type	1	0.68 ± 0.02
Activated; left shifted	PKA phosphorylated	2.3 ± 0.2***	0.11 ± 0.04***
	Ser-54 → Asp	2.9 ± 0.3***	0.07 ± 0.04***
	Ser-54 → Glu	2.0 ± 0.7**	0.09 ± 0.05***
Activated; right shifted	Glu-53 → Ala	2.5 ± 0.2***	1.1 ± 0.05**
	Ser-54 → Thr	0.94 ± 0.33†	0.64 ± 0.06†
Non-activated; not shifted	Ser-54 → Cys	1.03 ± 0.12†	0.42 ± 0.02**
	Ser-54 → Tyr	0.88 ± 0.21†	0.61 ± 0.05†
	Asp-53	1.1 ± 0.1†	0.67 ± 0.5†
	Ser-54 → Ala	0.94 ± 0.08†	0.09 ± 0.03***
	Ser-54 → Ile	1.0 ± 0.3†	0.08 ± 0.02***
Non-activated; left shifted	Ser-54 → Phe	1.3 ± 0.4†	0.05 ± 0.03***
	Ser-54 → Pro	0.99 ± 0.12†	0.09 ± 0.04***
	Ser-13 → Ala/Ser-54 → Ala	0.71 ± 0.22†	0.09 ± 0.02***
	Ser-54 → Gly	0.2 ± 0.3**	0.11 ± 0.08***
Inhibited; left shifted	Ser-54 → Arg	0.5 ± 0.2**	0.10 ± 0.02***
	Ser-13 → Ala	0.92 ± 0.12†	0.67 ± 0.06†
Ser-13 mutants non-activated; non-shifted	Ser-13 → Asp	1.05 ± 0.07†	0.68 ± 0.07†
	Arg-51 → Ala/Arg-52 → Ala	1.0 ± 0.2†	0.63 ± 0.3†

antibody specific for PDE4D species [18], generated against its C-terminal region, allowed us to identify both recombinant native and VSV tagged forms of PDE4D3 expressed in transiently transfected COS1 cells. Using identical amounts of immunoreactive species in PDE assays we were able to demonstrate that the relative (specific) activities of the two forms was identical (< 5% difference; *n* = 5). The tagged and non-tagged forms of PDE4D3 also showed similar K_m values for cAMP hydrolysis of 1.1 ± 0.2 μM and 0.9 ± 0.3 μM respectively, and had similar IC₅₀ values for inhibition by rolipram of 0.68 ± 0.07 μM and 0.66 ± 0.02 μM respectively (means ± S.D.; *n* = 5 separate analyses).

Such results indicate that the VSV epitope tag did not effect any gross changes in the apparent molecular mass or the enzymic activity of HSPDE4D3.

Activity analyses of HSPDE4D3 mutants

PKA phosphorylation of Ser-54 has been suggested [24,40] to lead to the activation of PDE4D3. In order to determine if the placement of a single negative charge at the position of Ser-54 could lead to increased enzyme activity we generated the Ser-54 → Asp mutant. Indeed, this mutant exhibited a specific activity that was ~ 3-fold higher than that of the wild-type enzyme (Table 1). Similarly, the Ser-54 → Glu mutant, which also analysed the effect of replacement of Ser-54 with a negatively charged amino acid, led to an increase in enzyme activity (Table 1). The magnitude of such increases in the activity of HSPDE4D3 were very similar to that which could be achieved by the phosphorylation of wild-type PDE4D3 through the action of PKA (Table 1).

Such an increase in activity of the Ser-54 → Asp mutant was uncoupled from any changes at Ser-13, the other site [23] for

PKA phosphorylation of PDE4D3, as PKA treatment of the Ser-54 → Asp mutant failed to elicit any change in activity (< 5% difference; *n* = 3), despite the fact that phosphorylation at Ser-13 ensued (see below). Consistent with this, PKA treatment of the Ser-13 → Asp mutant, which had a similar activity to the wild-type enzyme (Table 1), allowed for activation of this mutant enzyme (2.1 ± 0.3-fold; S.D. ± mean; *n* = 3) of a magnitude which was similar to that seen for the wild-type enzyme (Table 1).

The increased PDE activity seen for the Ser-54 → Asp mutant was highly specific, in that mutation to a variety of other amino acids, done in order to assess the effect of altering hydrophobicity, positive charge, aromatic group and helix disruption/distortion, failed to produce mutants with enzyme activities which were increased above that of the wild-type enzyme (Table 1). Indeed, a marked reduction in activity was seen with the Ser-54 → Gly and Ser-54 → Arg mutants. It is likely that these residues engender specific inhibitory conformational changes in the enzyme, as replacement with a number of other residues had little, if any, effect on enzyme activity (Table 1). This serves to support the notion that changes within the UCR1 region, in which Ser-54 lies and which forms a unique signature of long-form PDE4 species, can profoundly affect enzyme activity, presumably by generating changes in the conformation of the catalytic unit. It would thus appear that the PKA-mediated increase in activity of PDE4D3 can be mimicked by the Ser-54 → Asp mutant, suggesting that it is the placement of a negative charge at position 54 in the UCR1 region of HSPDE4D3 which triggers enzyme activation.

Phosphorylation analyses of mutant HSPDE4D3 species

We demonstrate here that in COS-1 cells, transfected so as to transiently express PDE4D3, a profound phosphorylation of this

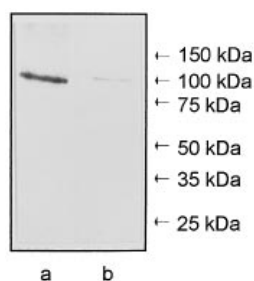


Figure 3 Phosphorylation of recombinant HSPDE4D3 by forskolin increased levels of cAMP in intact COS1 cells

Autoradiographs of immunoprecipitates of VSV epitope-tagged PDE4D3 from transfected ^{33}P -labelled COS1 cells subjected to SDS/PAGE as described in the Materials and methods section. Equal amounts of immunoreactive protein were loaded on each lane, with lane a, from cells treated with forskolin and lane b, from untreated cells.

enzyme occurred (Figure 3) upon increasing intracellular cAMP concentration using the adenylate cyclase activator forskolin [14,41].

In order to make comparative analyses of mutant enzymes under conditions where we could control the level of phosphorylation of the enzyme we employed an *in vitro* phosphorylation procedure using immunoprecipitates of epitope-tagged HSPDE4D3 which were incubated with the purified catalytic unit of PKA together with $[\gamma\text{-}^{33}\text{P}]\text{ATP}$. This treatment clearly led to the phosphorylation of the wild-type (Figure 4A), with maximum incorporation of label occurring after around 30 min of incubation (Figure 4B). No phosphorylation ensued if PKA was omitted from the incubation medium (results not shown).

That labelling occurred at the two consensus sites for PKA phosphorylation found in PDE4D3 was confirmed by the demonstration that no phosphorylation of the alanine double mutant, Ser-13 \rightarrow Ala/Ser-54 \rightarrow Ala occurred (Figure 4A). Furthermore, labelling was reduced by around a half using both of the single mutants Ser-54 \rightarrow Asp and Ser-54 \rightarrow Ala (Figure 4A) and also the Ser-13Ala and Ser-13 \rightarrow Asp mutants (results not shown). Sette and Conti [23] suggested that three other sub-optimal PKA consensus sequences in the N-terminal region of PDE4D3 might also serve as PKA phosphorylation sites. These imperfect PKA motifs form the amino acid sequence motif R/K(x)S, rather than the optimal sequence motif for PKA action of RRxS [42]. However, as we show here, PKA singularly failed (Figures 4A and 4C) to cause labelling of the alanine double mutant Ser-13 \rightarrow Ala/Ser-54 \rightarrow Ala, which clearly indicates that Ser-13 and Ser-54 provide the sole target sites for the PKA-mediated phosphorylation of native HSPDE4D3.

It is intriguing that Ser-54, which provides the PKA phosphorylation site associated with increased activity of this isoform, lies within a motif (RRRES) which contains a glutamate residue at position 53. On the basis of peptide studies, this negatively charged species can be expected to reduce the efficiency with which Ser-54 would be phosphorylated by PKA action [42]. In order to address whether this may hold true in a real protein, we generated the mutant species Glu-53 \rightarrow Ala so as to remove the negatively charged glutamate at position 53 in the PKA consensus site within which Ser-54 lies. So as to determine whether the Glu-53 \rightarrow Ala mutant would be phosphorylated more rapidly than the wild-type enzyme we compared the labelling of these species some 15 min after exposure to PKA; a time at which labelling of the wild-type enzyme was substantially

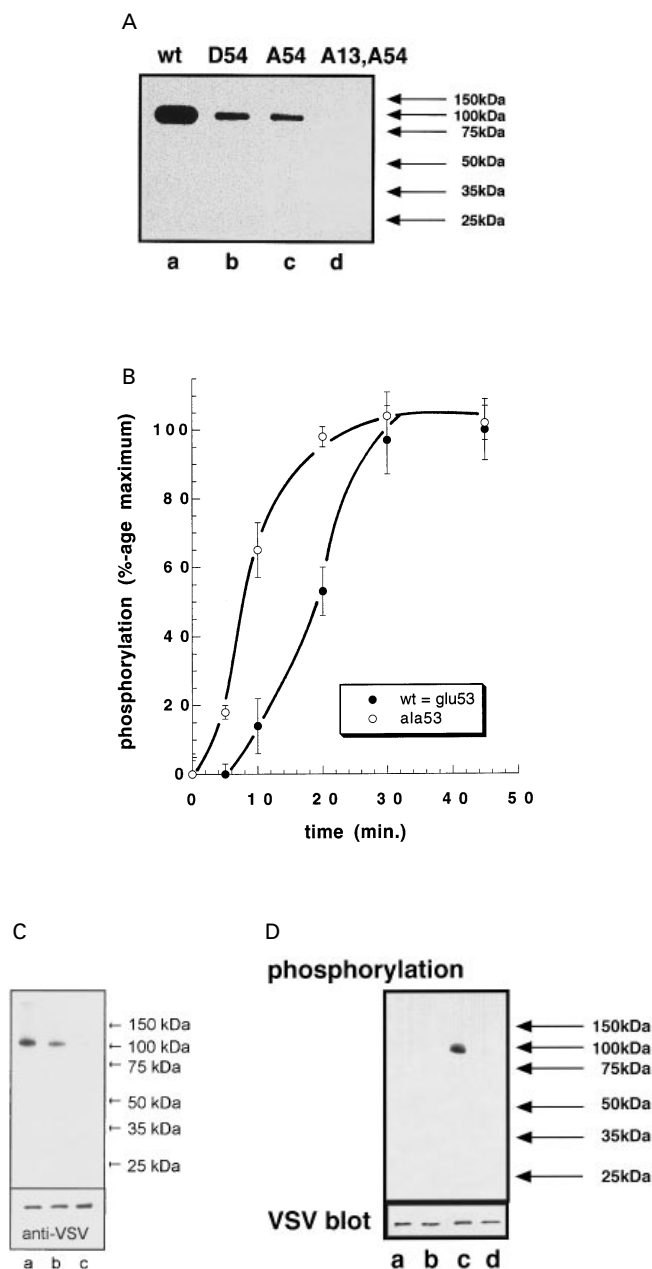


Figure 4 Phosphorylation of wild-type and mutant forms of HSPDE4D3 by PKA

(A) Autoradiographs of ^{33}P -labelled HSPDE4D3 species analysed by SDS/PAGE. Lane a, wild-type HSPDE4D3; lane b, Ser-54 \rightarrow Asp mutant; lane c, Ser-54 \rightarrow Ala mutant; and lane d, the Ser-13 \rightarrow Ala/Ser-54 \rightarrow Ala double mutant. Identical amounts of immunoreactive PDE4D3 were loaded onto each lane and thus the degree of labelling is directly comparable. In these studies, incubation with PKA was performed for 30 min. Data are typical of experiments done three times. (B) Time course of labelling of the wild-type HSPDE4D3 (●) and the Glu-53 \rightarrow Ala (○) mutant. Labelling is shown as a percentage of the maximum level achieved with results given as means \pm S.D. for $n = 3$ separate experiments. However, maximal labelling, assessed after 45 min exposure to PKA, was identical in all the experiments ($< 5\%$ difference; $n = 3$ experiments). (C) Autoradiographs of ^{33}P -labelled HSPDE4D3 species analysed by SDS/PAGE. Lane a, Glu-53 \rightarrow Ala mutant; lane b, wild-type enzyme; and lane c, Ser-13 \rightarrow Ala/Glu-54 \rightarrow Ala double mutant. In this instance incubation with PKA was performed for 15 min only. Results are typical of experiments done three times. (D) Autoradiographs of ^{33}P -labelled HSPDE4D3 species analysed by SDS/PAGE. Lane a, the triple mutant Ser-13 \rightarrow Ala/Glu-53 \rightarrow Ala/Ser-54 \rightarrow Ala; lane b, Ser-13 \rightarrow Ala/Ser-54 \rightarrow Ala double mutant; lane c, Glu-53 \rightarrow Asp mutant; and lane d, Ser-13 \rightarrow Ala/Arg-51 \rightarrow Ala/Arg-52 \rightarrow Ala triple mutant. In these studies incubation with PKA was performed for 30 min. Results are typical of experiments done three times.

reduced. Under such conditions we observed (Figure 4C) a considerably greater labelling of the Glu-53 → Ala mutant compared with the wild-type enzyme, suggesting that PKA phosphorylation of the Glu-53 → Ala mutant occurred much more rapidly than that of the wild-type enzyme. A detailed analysis of the time course of phosphorylation indicated that this was in fact the case (Figure 4B). Indeed, the half times for maximal labelling were 20 ± 3 min for the native enzyme and some 8 ± 2 min for the Glu-53 → Ala mutant ($n = 3$; mean \pm S.D.). The increase in labelling of the Glu-53 → Ala mutant was not due to the exposure of any 'latent' sites for PKA-mediated phosphorylation, as we failed to see any labelling of the alanine triple mutant, Ser-13 → Ala/Glu-53 → Ala/Ser-54 → Ala, where the two PKA sites in the native enzyme, namely Ser-13 and Ser-54, were destroyed by mutation of the serine targets to alanine (Figure 4D). Furthermore, prolonged incubation of the Glu-53 → Ala mutant with PKA led to similar levels of labelling to that seen with the wild-type enzyme (Figure 4B). Thus mutation of Glu-53 to Ala-53 appears to make HSPDE4D3 a better substrate for phosphorylation by PKA.

It is intriguing that the efficiency of action of PKA in phosphorylating Ser-54 in PDE4D3 should, apparently, be compromised by the consensus motif for PKA containing the negatively charged Glu-53. The explanation for this appears to be that Glu-53 has an essential role in the molecular events which lead to enzyme activation. This was deduced from our observation (Table 1) that the Glu-53 → Ala mutant exhibited an enhanced activity which was comparable with that exhibited by both the Ser-54 → Asp and phosphorylated wild-type enzyme. Not only this, but despite the Glu-53 → Ala mutant being more efficiently phosphorylated by PKA (Figures 4B and 4C), it was singularly insensitive to activation by PKA. Thus, under conditions of maximal PKA-mediated phosphorylation, we noted the activity of the phosphorylated Glu-53 → Ala mutant was some $96 \pm 5\%$ (mean \pm S.D.; $n = 3$) of that of the untreated Glu-53 → Ala mutant enzyme (100%). The enhanced activity of the Glu-53 → Ala mutant appeared to be related to loss of a negative charge at position 53, as the activity of the Glu-53 → Asp mutant, generated to conserve the negative charge at this position, was unchanged from that of the wild-type (Glu-53) enzyme (Table 1). Furthermore, this Glu-53 → Asp mutant could be phosphorylated by PKA (Figure 4D) in a manner which led to enzyme activation (1.9 ± 0.2 ; mean \pm S.D., $n = 3$) to a similar extent to that seen using the wild-type enzyme (Table 1). The increase in activity seen with the Glu-53 → Ala mutant was highly specific for this position in HSPDE4D3, as no activation was seen with the Ser-54 → Ala mutant (Table 1); neither was any activation seen with the Arg-51 → Ala/Arg-52 → Ala double mutant whose activity was similar ($98 \pm 5\%$; means \pm S.D.; $n = 3$) to that of the wild-type enzyme (100%). These observations militate against any non-specific disruption having led to the profound increase in activity seen with the Glu-53 → Ala mutant.

Disruption of the Ser-54 consensus site (RRES⁵⁴) by mutation to alanine of both Arg-51 and Arg-52 clearly prevented PKA from causing phosphorylation at Ser-54, as seen in the failure of PKA to cause any labelling whatsoever of the triple mutant Ser-13 → Ala/Arg-51 → Ala/Arg-52 → Ala (Figure 4D). Indeed, the activity of the Arg-51 → Ala/Arg-52 → Ala double mutant was not stimulated by PKA treatment, being $96 \pm 7\%$ (mean \pm S.D.; $n = 3$) of that of the untreated enzyme, despite this species being phosphorylated at Ser-13 by PKA action.

Thus, it would seem that the negatively charged Glu-53 residue in PDE4D3 plays a key role in the PKA-mediated activation process. One possible explanation for this is that such a residue

may be involved in forming an ion-pair which holds the enzyme in an attenuated state and whose disruption leads to activation. This could be envisaged to ensue either from the placement of a bulky negatively charged group at Ser-54, effected by PKA-mediated phosphorylation, or by mutation to remove the negatively charged Glu-53. Such a model would explain the failure of the Glu-53 → Ala mutant to be activated by PKA-mediated phosphorylation.

Inhibition of HSPDE4D3 by rolipram

The compound rolipram has both anti-depressant and anti-inflammatory actions and serves as a highly selective PDE4 inhibitor [6,9,10,12,43–48]. Rolipram has been shown to display a wide range of inhibitory potencies, at concentrations varying from 0.2 to $2 \mu\text{M}$, against natively expressed, crude PDE4 enzyme preparations (e.g. see for discussion [6,10,12]). It has been suggested [6] that such disparity is not simply due to differences in PDE4 isoform expression, as rolipram does not appear to show any simple pattern of discrimination for inhibition of the various PDE4 isoform classes. Indeed, for the same PDE4 isoform, differences in sensitivity to inhibition have been observed, dependent upon the cell background the recombinant enzyme is expressed in as well as the subcellular fraction in which it is located [18,33,38,49]. It has been suggested, on the basis of substrate kinetic studies [50], that at least certain PDE4 isoforms might exist in interconvertible states, and that certain conformations can be discriminated by different sensitivities to inhibition by rolipram [6,11]. The notion that rolipram could serve to identify different PDE4 conformers first arose from observations [51] that the PDE4 activity associated with guinea pig eosinophil membranes showed a dramatic increase in sensitivity to inhibition by rolipram upon either solubilization or treatment with vanadyl–glutathione complexes. The converse observation has been made for a recombinant PDE4A isoform, where it has been demonstrated [33] that the expression of HSPDE4A4B in COS7 cells led to the expression of not only a soluble cytosolic enzyme but also a particulate enzyme whose kinetics of inhibition by rolipram changed in a manner consistent with the enzyme having undergone a conformational change upon interaction with subcellular structures. This resulted in an increased sensitivity to inhibition of the particulate enzyme by rolipram, as indicated by a decrease in the IC_{50} value for inhibition compared with the cytosol-expressed component of this isoform. Studies on recombinant HSPDE4D3 have led to the suggestion that PKA-mediated phosphorylation of this enzyme might elicit a physiological change in its conformation that can be detected by rolipram [24]. It thus appears that the conformational status of members of the PDE4 enzyme family may be subject to modulation by a variety of cellular processes which are likely to be of fundamental importance to their function. Rolipram is one of a number of PDE4-selective inhibitors that can discriminate between certain of these conformational states. Despite rolipram being a competitive inhibitor, such changes do not appear to be correlated with any alteration in the K_m for cAMP. This suggests that rolipram can bind to regions within the catalytic site which do not influence the binding of cAMP. Consistent with this notion, it has been shown that mutant PDE4 enzymes can be generated which are not inhibited by rolipram, yet show no change in the K_m for cAMP [52].

Using recombinant HSPDE4D3 expressed in COS-1 cells, we show here (Table 1) that PKA phosphorylation of this enzyme clearly lowered the IC_{50} value for rolipram inhibition. Furthermore, as with enzyme activation, such a change was mimicked (Table 1; Figure 5A) by the Ser-54 → Asp mutant. In contrast,

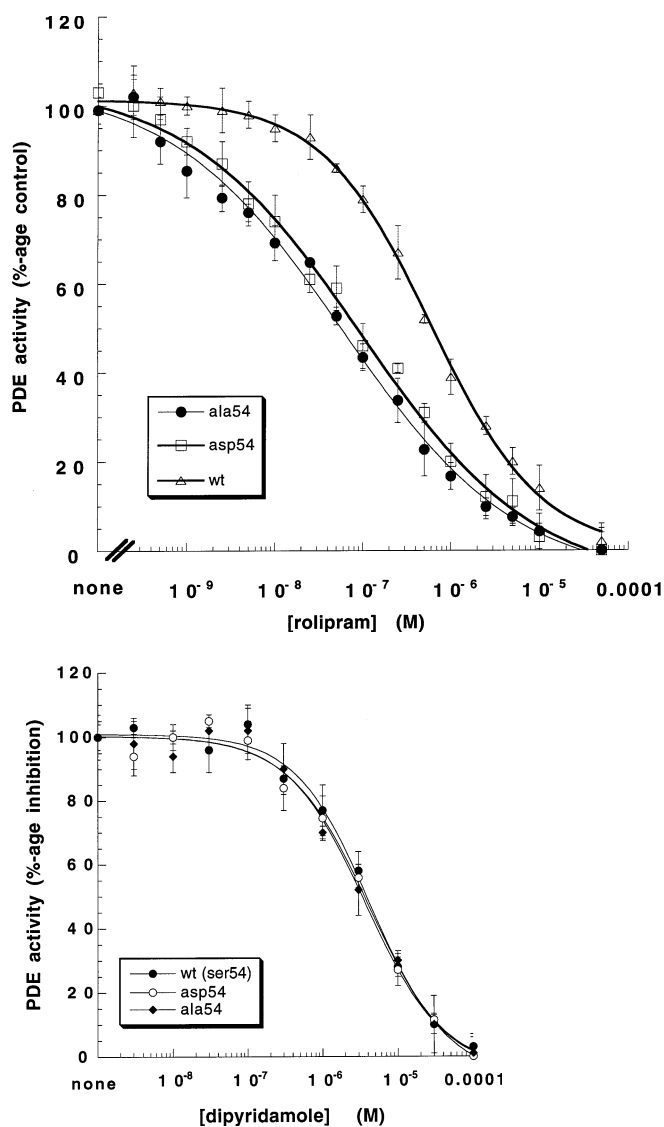


Figure 5 Inhibition of HSPDE4D3 activity by rolipram

Dose-effect plots for the inhibition of cAMP PDE activity. Top: action of rolipram on wild-type HSPDE4D3 (Δ) and the two mutant HSPDE4D3 forms Ser-54 \rightarrow Asp (\square) and Ser-54 \rightarrow Ala (\bullet) species. Bottom: action of dipyrindamole on wild-type HSPDE4D3 (\bullet) and the two mutant HSPDE4D3 forms Ser-54 \rightarrow Asp (\circ) and Ser-54 \rightarrow Ala (\blacklozenge) species. Assays were performed using $1 \mu\text{M}$ cAMP as substrate. These results are means \pm S.D. of $n = 3$ experiments.

no such change in rolipram inhibition was evident using the Ser-13 \rightarrow Asp mutant (Table 1), indicating that the change in rolipram inhibition was specific to modification at residue 54. Such results clearly show that for recombinant HSPDE4D3 expressed in COS-1 cells it is possible to achieve a marked increase in sensitivity to rolipram inhibition through PKA-mediated phosphorylation. This means that in cells where cAMP levels are elevated to a level able to activate PKA then the rolipram inhibition characteristics of PDE4D3 will be changed.

It was intriguing to note a similar decrease in the IC_{50} value for inhibition by rolipram when analysing the properties of a variety of residue-54 mutant HSPDE4D3 species which did not elicit enzyme activation (Table 1; Figure 5A). Such observations suggest that the conformational change which leads to altered rolipram inhibition can be dissociated from that which causes

enzyme activation. Further support for such a notion comes from the fact that, whereas the Ser-53 \rightarrow Ala mutant effected a profound increase in enzyme activity, this occurred without any accompanying increase in sensitivity to rolipram inhibition (Table 1). Nevertheless, we observed that the Ser-54 \rightarrow Thr mutant exhibited a sensitivity to inhibition by rolipram which matched that of the wild-type (Ser-54) enzyme (Table 1). Both serine and threonine have side-chain hydroxy groups which can serve as hydrogen-bond donors. We suggest that a possible explanation for this is that the side-chain hydroxy of Ser-54 may be involved in hydrogen-bonding with a residue which stabilizes a particular conformation of HSPDE4D3 and whose disruption triggers a conformational change in this enzyme which is detected by an enhanced sensitivity to inhibition by rolipram. Consistent with such a proposal is that inhibition by rolipram was little altered (Table 1) in the Ser-54 \rightarrow Cys mutant, whose thiol side-chain can serve as a weak hydrogen-bond donor. Neither was rolipram inhibition altered in the Ser-54 \rightarrow Tyr mutant, which like the native Ser-54 enzyme has a residue at position 54 with a side-chain hydroxy group able to undergo hydrogen-bonding. Here we suggest a model (Figure 6) in which the disruption of a putative hydrogen-bond involving the side-chain hydroxy group of Ser-54 would cause a conformational change in the catalytic unit of the enzyme, which is detected by an increase in sensitivity to rolipram inhibition without causing enzyme activation. This would explain why substitution at position 54 with various amino acids whose side-chains are unable to serve as hydrogen-bond donors led to an increased sensitivity to rolipram inhibition without causing enzyme activation (Table 1).

Analyses done on PDE4 enzyme preparations from various cells where these enzymes are expressed natively has demonstrated a wide range of different IC_{50} values for rolipram inhibition [6]. In some such instances, increased sensitivity to inhibition by rolipram led to an ability of enzyme preparations to discriminate between the two enantiomeric forms, $R(-)$ and $S(+)$, of rolipram [6,53,54]. The analyses reported above were done using a racemic mixture of rolipram enantiomers. Using the separate enantiomers, the wild-type enzyme showed little discrimination between them, with IC_{50} values of 0.63 ± 0.05 and $0.57 \pm 0.03 \mu\text{M}$ for R and S rolipram respectively ($n = 3$; means \pm S.D.). In contrast, the Ser-54 \rightarrow Asp mutant yielded IC_{50} values of 0.05 ± 0.03 and $0.18 \pm 0.03 \mu\text{M}$ for $R(-)$ and $S(+)$ rolipram respectively ($n = 3$; means \pm S.D.). Thus the ratio of the IC_{50} values for inhibition by these two enantiomers (S/R value) rose from 0.9 for the wild-type to 3.6 for the Ser-54 \rightarrow Asp mutant. In contrast with this, the Ser-54 \rightarrow Tyr mutant, which like the native enzyme has a side-chain hydroxy group at position 54, exhibited similar IC_{50} values of 0.62 ± 0.04 and $0.62 \pm 0.03 \mu\text{M}$ for $R(-)$ and $S(+)$ rolipram respectively ($n = 3$; means \pm S. D.).

Studies on natively expressed PDE4 preparations have also identified compounds which do not appear to be capable of discriminating between forms of the enzyme which show different susceptibilities to inhibition by rolipram. An example of such a compound is dipyrindamole [6]. Here we show (Figure 5B) that the wild-type HSPDE4D3, as well as the Ser-54 \rightarrow Ala and Ser-54 \rightarrow Asp mutants, were all similarly inhibited by dipyrindamole, with IC_{50} values of 4.1 ± 0.6 , 4.5 ± 0.6 and $4.0 \pm 0.5 \mu\text{M}$ respectively ($n = 3$; means \pm S.D.). Such values are similar to that of $5.2 \mu\text{M}$ observed for the inhibition of recombinant HSPDE4A by dipyrindamole [53].

These various experiments add further support to the contention that the Ser-54 \rightarrow Asp mutant accurately mimics a stoichiometrically PKA phosphorylated and activated population of HSPDE4D3. This mutant has apparently undergone a

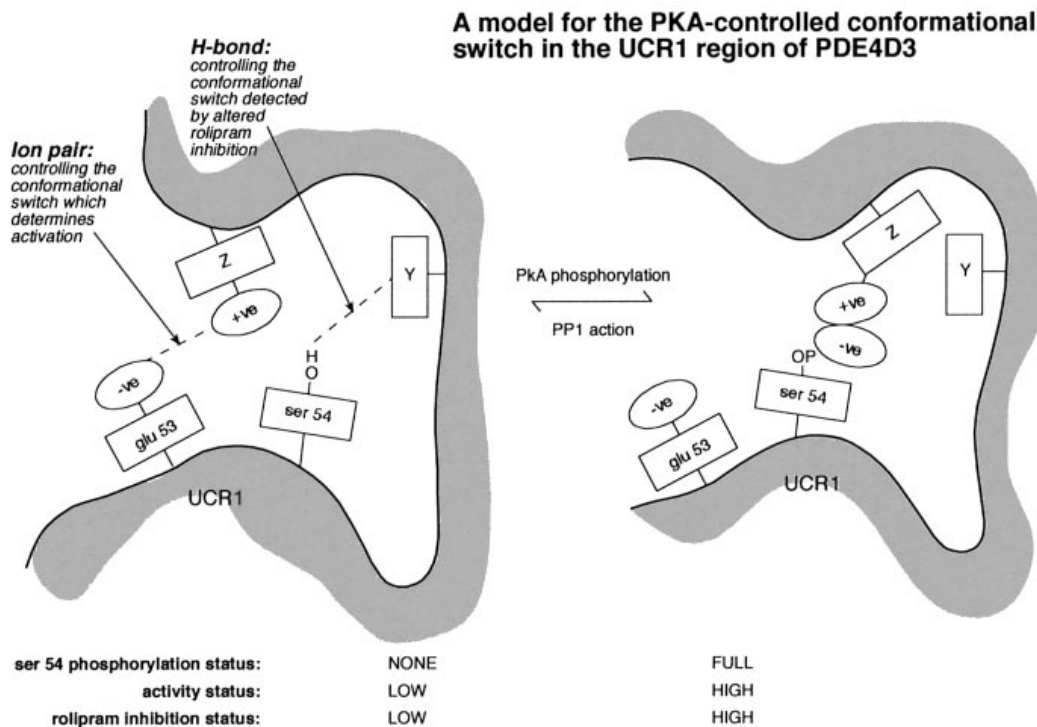


Figure 6 Model for the conformational changes invoked in HSPDE4D3 by PKA-mediated phosphorylation of Ser-54

This schematic diagram envisages that the side-chain hydroxy group of Ser-54 serves as a hydrogen-bond donor and thus interacts with an unidentified residue shown as 'Y', and that Glu-53 is involved in an ion-pair with an unidentified residue shown as 'Z'. Disruption of the putative hydrogen-bond is suggested to lead to a change in conformation of the catalytic unit of the enzymes, which is detected by an increase in sensitivity to inhibition by rolipram, but not by activation. This is exemplified by the Ser-54 → Ala mutant. Disruption of the putative ion-pair is suggested to lead to a conformational change in the catalytic unit, which causes activation but does not show enhanced sensitivity to rolipram inhibition. This is exemplified by the Glu-53 → Ala mutant. Disruption of both interactions is suggested to lead to both enzyme activation and increased sensitivity to rolipram inhibition. This requires the placement of a negative charge at residue position 54 and is exemplified either by PKA-mediated phosphorylation of Ser-54 or by the Ser-54 → Asp mutant. One possible explanation for activation occurring in this instance is that the negative charge placed at position 54 might disrupt the ion-pair involving Glu-53, perhaps by competing for the cationic acceptor (as seen in this schematic diagram), or causing a conformational change which disrupts the ion-pair involving Glu-53.

conformational change in addition to that which causes activation, and this is detected by a change in its sensitivity to inhibition by rolipram. The observation that, compared with native HSPDE4D3, the Ser-54 → Asp mutant exhibits an ability to discriminate between *R*(-) and *S*(+) rolipram, shows heightened sensitivity to inhibition by rolipram and identical sensitivity to inhibition by dipyridamole, suggests that PKA-modified HSPDE4D3 may provide at least a fraction of the PDE4 component that is found expressed natively and which exhibits a high-affinity interaction with rolipram.

Conclusions

Whereas the three-dimensional structure of HSPDE4D3 is unknown, sequence analysis has identified a central catalytic region of ~ 357 residues. Upstream of this are two regions which provide unique signatures of long-form PDE4 products and are known as the UCR1 region, of 55 residues, and the UCR2 region, of 76 residues (see e.g. [10]). The finding of Conti and co-workers [23,24] that the PKA-mediated phosphorylation of Ser-54, which is located within the UCR1 region of PDE4D3, led to enzyme activation, suggests that changes in the conformation of UCR1 might trigger conformational changes in the catalytic domain of the enzyme. Our results, using mutant forms of HSPDE4D3, adds substance to such a notion and indicates that Ser-54 may serve as a conformational switch which is operated

by PKA-mediated phosphorylation. We suggest that the side-chain hydroxy of Ser-54 may be involved in hydrogen-bonding to an as yet unidentified residue, and that disruption of this bond triggers a change in the conformation of the catalytic unit which is detected by an enhanced susceptibility of the enzyme to inhibition by rolipram.

However, our studies indicate that the disruption of such a putative hydrogen-bond is insufficient to cause enzyme activation. Rather, the activation of HSPDE4D3 appears to require the placement of a negative charge at position 54 in the protein. Physiologically, this is effected by the PKA-mediated phosphorylation of Ser-54, although we show here that such an effect can be mimicked by mutation of the Ser-54 in the native enzyme to either of the negatively charged amino acids aspartate or glutamate (Table 1).

Our intriguing observation that the Glu-53 → Ala mutant produced an activated enzyme, with accompanying loss in the ability of PKA to activate, but not to phosphorylate, HSPDE4D3, has led us to suggest that, in the native enzyme, Glu-53 might be involved in forming an ion-pair with a positively charged residue, and that it is the disruption of such a bond that is responsible for triggering enzyme activation. On this basis, we propose that activation by PKA is caused by the placement of a large, negatively charged, phosphate group in association with the side-chain of Ser-54, which disrupts the ion-pair involving Glu-53. This may ensue because the phosphate group competes

more effectively for the cationic species proposed to interact with Glu-53 in the ground state of the enzyme (Figure 6). Such a process would be expected to be mimicked by the Ser-54 → Asp and Ser-54 → Glu mutant forms. In addition, in such activated mutant enzymes the loss of the side-chain hydroxy group of Ser-54 would also be expected to disrupt the putative hydrogen-bond involving this residue, yielding an associated increase in sensitivity to inhibition by rolipram (Figure 5b). Such a model implies that residues in the UCR1 region of HSPDE4D3 may interact with other regions of the protein, implying a functional significance for this region which forms a unique signature that characterizes long-form PDE4 isoforms.

Our analyses, employing various mutant forms of HSPDE4D3, clearly show that it is possible to 'uncouple' the conformational change in the catalytic unit, which leads to alterations in sensitivity to inhibition by rolipram, from that leading to activation of this particular isoform. The ability to generate mutants which mimic distinct conformational states of HSPDE4D3 may provide useful screens for developing inhibitors which can select between the various functional states of this isoform. They also overcome the difficulty of generating enzymes for analysis which reflect the true ground-state of the enzyme, where none of the enzyme population is phosphorylated at Ser-54, and a fully activated state, where all of the enzyme population is phosphorylated at Ser-54. We suggest that the Ser-54 → Asp mutant provides a good model of the fully activated (phosphorylated) enzyme with altered rolipram inhibition, and that the Arg-51 → Ala/Arg-52 → Ala double mutant is the best model of the ground-state enzyme, as it cannot be phosphorylated at Ser-54 by PKA action due to the disruption of the consensus site and, furthermore, it does not exhibit altered sensitivity to inhibition by rolipram, as is evident, for example, with the Ser-54 → Ala mutant. Such mutant forms of HSPDE4D3 are likely to be of use in defining the function of this isoform in modulating cell-signalling processes and as stable species suitable for identifying novel inhibitors which can discriminate between conformationally distinct states of this isoform.

This work was supported by a grant from the Medical Research Council to M.D.H. and also by a Wellcome Trust capital equipment grant to M.D.H. We thank M. Stefani for technical assistance and A. Wanner for sequencing work. We also appreciate helpful discussions with Dr. J. Fozard, Dr. E. Tobias and Dr. H. W. Hofer.

REFERENCES

- Houslay, M. D. and Milligan, G. (1997) *Trends Biochem. Sci.* **22**, 217–224
- Beavo, J. A. (1995) *Physiol. Rev.* **75**, 725–748
- Conti, M., Nemoz, G., Sette, C. and Vicini, E. (1995) *Endocrinol. Rev.* **16**, 370–389
- Bolger, G. (1994) *Cell. Signalling* **6**, 851–859
- Manganiello, V. C., Murata, T., Taira, M., Belfrage, P. and Degerman, E. (1995) *Arch. Biochem. Biophys.* **322**, 1–13
- Souness, J. E. and Rao, S. (1997) *Cell. Signalling* **9**, 227–236
- Torphy, T. J., Udem, B. J., Cieslinski, L. B., Luttmann, M. A., Reeves, M. L. and Hay, D. W. P. (1993) *J. Pharmacol. Exp. Ther.* **265**, 1213–1223
- Thompson, W. J. (1991) *Pharmacol. Ther.* **51**, 13–33
- Dent, G. and Giembycz, M. A. (1995) *Clin. Immunother.* **3**, 423–437
- Houslay, M. D., Sullivan, M. and Bolger, G. B. (1997) *Adv. Pharmacol.* **44**, 225–342
- Torphy, T. J., Dewolf, W., Green, D. W. and Livi, G. P. (1993) *Agents Actions* **43**, 51–71
- Torphy, T. J., Barnette, M. S., Hay, D. W. P. and Underwood, D. C. (1994) *Environ. Health Perspect.* **102**, 79–84
- Torphy, T. J., Livi, G. P. and Christensen, S. B. (1993) *Drug News Perspect.* **6**, 203–214
- Houslay, M. D., Scotland, G., Erdogan, S., Huston, E., Mackenzie, S., McCallum, J. F., McPhee, I., Pooley, L., Rena, G., Ross, A., et al. (1997) *Biochem. Soc. Trans.* **25**, 374–381
- Houslay, M. D. (1996) *Biochem. Soc. Trans.* **24**, 980–986
- Bolger, G., Michaeli, T., Martins, T., St. John, T., Steiner, B., Rodgers, L., Riggs, M., Wigler, M. and Ferguson, K. (1993) *Mol. Cell. Biol.* **13**, 6558–6571
- Bolger, G. B., Rodgers, L. and Riggs, M. (1994) *Gene* **149**, 237–244
- Bolger, G. B., Erdogan, S., Jones, R. E., Loughney, K., Scotland, G., Hoffmann, R., Wilkinson, I., Farrell, C. and Houslay, M. D. (1997) *Biochem. J.* **328**, 539–548
- Conti, M., Swinnen, J. V., Tsikalas, K. E. and Jin, S. L. C. (1992) *Adv. Second Messenger Phosphoprotein Res.* **25**, 87–99
- Sette, C., Vicini, E. and Conti, M. (1994) *J. Biol. Chem.* **269**, 18271–18274
- Sette, C., Vicini, E. and Conti, M. (1994) *Mol. Cell. Endocrinol.* **100**, 75–79
- Conti, M., Iona, S., Cuomo, M., Swinnen, J. V., Odeh, J. and Svoboda, M. E. (1995) *Biochemistry* **34**, 7979–7987
- Sette, C. and Conti, M. (1996) *J. Biol. Chem.* **271**, 16526–16534
- Alvarez, R., Sette, C., Yang, D., Eglon, R. M., Wilhelm, R., Shelton, E. R. and Conti, M. (1995) *Mol. Pharmacol.* **48**, 616–622
- Bradford, M. (1976) *Anal. Biochem.* **72**, 248–254
- Laemmli, U. K. (1970) *Nature (London)* **222**, 680–682
- Wilkinson, I., Engels, P. and Houslay, M. D. (1997) *Pharmacol. Rev. Commun.* **9**, 215–226
- Kreis, T. E. and Lodish, H. F. (1986) *Cell* **46**, 929–937
- Soldati, T. and Perriard, J. C. (1991) *Cell* **66**, 277–289
- Thompson, W. J. and Appleman, M. M. (1971) *Biochemistry* **10**, 311–316
- Rutten, W. J., Schoot, B. M. and Dupont, J. S. H. (1973) *Biochim. Biophys. Acta* **315**, 378–383
- Marchmont, R. J. and Houslay, M. D. (1980) *Biochem. J.* **187**, 381–392
- Huston, E., Pooley, L., Julien, J., Scotland, G., McPhee, I., Sullivan, M., Bolger, G. and Houslay, M. D. (1996) *J. Biol. Chem.* **271**, 31334–31344
- McPhee, I., Pooley, L., Lobban, M., Bolger, G. and Houslay, M. D. (1995) *Biochem. J.* **310**, 965–974
- Bolger, G., McPhee, I. and Houslay, M. D. (1996) *J. Biol. Chem.* **271**, 1065–1071
- Shakur, Y., Pryde, J. G. and Houslay, M. D. (1993) *Biochem. J.* **292**, 677–686
- Shakur, Y., Wilson, M., Pooley, L., Lobban, M., Griffiths, S. L., Campbell, A. M., Beattie, J., Daly, C. and Houslay, M. D. (1995) *Biochem. J.* **306**, 801–809
- Huston, E., Lumb, S., Russell, A., Catterall, C., Ross, A. H., Steele, M. R., Bolger, G. B., Perry, M., Owens, R. and Houslay, M. D. (1997) *Biochem. J.* **328**, 549–558
- Lobban, M., Shakur, Y., Beattie, J. and Houslay, M. D. (1994) *Biochem. J.* **304**, 399–406
- Sette, C., Iona, S. and Conti, M. (1994) *J. Biol. Chem.* **269**, 9245–9252
- Tang, W. J. and Gilman, A. G. (1995) *Science* **268**, 1769–1772
- Kemp, B. E. and Pearson, R. B. (1990) *Trends Biochem. Sci.* **15**, 342–346
- Dent, G. and Giembycz, M. A. (1996) *Thorax* **51**, 647–649
- Wachtel, H. (1983) *Neuropharmacology* **22**, 267–272
- Lowe, J. A. and Cheng, J. B. (1992) *Drugs Future* **17**, 799–807
- Barnette, M. S., Christensen, S. B., Underwood, D. C. and Torphy, T. J. (1996) *Pharmacol. Commun.* **8**, 65–73
- Banner, K. H. and Page, C. P. (1995) *Eur. Respir. J.* **8**, 996–1000
- Teixeira, M. M., Gristwood, R. W., Cooper, N. and Hellewell, P. G. (1997) *Trends Pharmacol. Sci.* **18**, 164–170
- Owens, R. J., Lumb, S., Rees-Milton, K., Russell, A., Baldock, D., Lang, V., Crabbe, T., Ballesteros, M. and Perry, M. J. (1997) *Cell. Signalling* **9**, 575–585
- Marchmont, R. J., Ayad, S. R. and Houslay, M. D. (1981) *Biochem. J.* **195**, 645–652
- Souness, J. E., Maslen, C. and Scott, L. C. (1992) *FEBS Lett.* **302**, 181–184
- Pillai, R., Kytte, K., Reyes, A. and Colicelli, J. (1993) *Proc. Natl. Acad. Sci. U.S.A.* **90**, 11970–11974
- Torphy, T. J., Stadel, J. M., Burman, M., Cieslinski, L. B., McLaughlin, M. M., White, J. R. and Livi, G. P. (1992) *J. Biol. Chem.* **267**, 1798–1804
- Souness, J. E. and Scott, L. C. (1993) *Biochem. J.* **291**, 389–395